Sub-70 nm extreme ultraviolet lithography at the Advanced Light Source static microfield exposure station using the engineering test stand set-2 optic

Patrick Naulleau,[a] Kenneth A. Goldberg, and Erik H. Anderson
Center for X-Ray Optics, Lawrence Berkeley National Laboratory, Berkeley, California 94720

David Attwood
EECS Department, University of California, Berkeley, California 94720

Phillip Batson
Center for X-Ray Optics, Lawrence Berkeley National Laboratory, Berkeley, California 94720

Jeffrey Bokor
Center for X-Ray Optics, Lawrence Berkeley National Laboratory and EECS Department, University of California, Berkeley, California 94720

Paul Denham, Eric Gullikson, Bruce Harteneck, Brian Hoef, Keith Jackson, Deirdre Olynick, Seno Rekawa, and Farhad Salmassi
Center for X-Ray Optics, Lawrence Berkeley National Laboratory, Berkeley, California 94720

Ken Blaedel, Henry Chapman, Layton Hale, Paul Mirkarimi, Regina Soufli, Eberhard Spiller, Don Sweeney, John Taylor, and Chris Walton
Lawrence Livermore National Laboratory, P. O. Box 808, Livermore, California 94550

Donna O'Connell and Daniel Tichenor
Sandia National Laboratories, P. O. Box 969, Livermore, California 94551

Charles W. Gwyn, Pei-Yang Yan, and Guojing Zhang
Intel Corporation, 2200 Mission College Boulevard, Santa Clara, California 95052

(Received 28 May 2002; accepted 7 October 2002)

Static microfield printing capabilities have recently been integrated into the extreme ultraviolet interferometer operating at the Advanced Light Source synchrotron radiation facility at Lawrence Berkeley National Laboratory. The static printing capabilities include a fully programmable scanning illumination system enabling the synthesis of arbitrary illumination coherence (pupil fill). This new exposure station has been used to lithographically characterize the static imaging performance of the Engineering Test Stand Set-2 optic. Excellent performance has been demonstrated down to the 70 nm equal line/space level with focus latitude exceeding 1 μm and dose latitude of approximately 10%. Moreover, equal line/space printing down to a resolution of 50 nm has been demonstrated using resolution-enhancing pupil fills. © *2002 American Vacuum Society.*
[DOI: 10.1116/1.1524976]

I. INTRODUCTION

Extreme ultraviolet (EUV) projection lithography is now the leading contender for next-generation lithography beyond the limits imposed by current refractive optical systems. Because EUV systems utilize resonant reflective coatings,[1] at-wavelength characterization,[2] including system wavefront metrology,[3,4] has played an essential role in the development of EUV lithographic optics.

While interferometry is routinely used for the characterization and alignment of lithographic optics, the ultimate performance metric for these optical systems is image transfer to photoresist. Moreover, the comparison of lithographic imaging with that predicted from wave front performance is also useful for verifying and improving the predictive power of wave front metrology. To address these issues, static, microfield printing capabilities have been added to the EUV phase-shifting point diffraction interferometer (PS/PDI) implemented at the Advanced Light Source synchrotron radiation facility at Lawrence Berkeley National Laboratory.[3,4] The metrology station was developed to align and characterize lithographic-quality four-mirror optical systems[5] designed for use in the EUV engineering Test Stand (ETS) prototype stepper.[6] The static printing capabilities include a 100 μm field at the wafer as well as the ability to cover the full optic field of view one microfield at a time by moving the entire system relative to the stationary illumination beam. The compound metrology station remains flexible, and switching between interferometry and imaging modes can be accomplished in approximately 2 weeks.

Relevant printing studies with the lithographic optics of concern here require partially coherent illumination with a coherence factor σ of approximately 0.7. We note however, that this σ value is very different from the high degree of

[a]Present address: LBNL, MS2-400, 1 Cyclotron Rd., Berkeley, CA 94720; electronic mail: Pnaulleau@lbl.gov

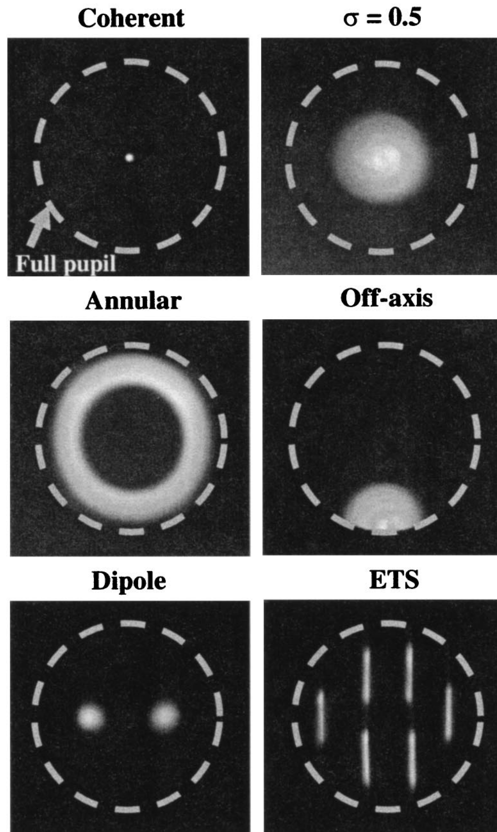

FIG. 1. Series of EUV pupil fills generated by the scanning system and recorded through the lithographic ETS Set-2 optic. A back-thinned back-illuminated EUV CCD camera is used to capture the pupil-fill images.

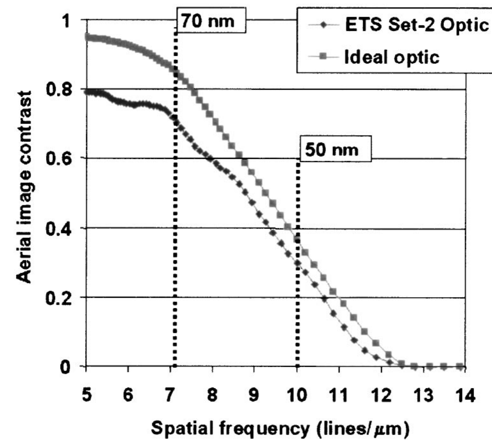

FIG. 2. Calculated binary-dense-line modulation transfer function (MTF) at the central field point assuming a partial coherence of 0.7.

coherence required for high accuracy EUV interferometry and that which is naturally generated by the synchrotron undulator beamline.[7,8] Adding printing capabilities to the PS/PDI experimental system has thus necessitated the development of an alternative illumination system capable of modifying the inherent coherence of the beamline. The implemented illuminator is an angular scanning illuminator[9–11] capable of *in situ* coherence control. Moreover, this flexible scanning illuminator design readily enables the generation of arbitrary, customizable pupil fills, including resolution enhancing pupil fills and modeling of stepper-specific pupil fills such as the ETS six-channel design.[6]

The static microfield exposure station integrated into the EUV PS/PDI has been used to lithographically characterize the static imaging performance of the ETS Set-2 projection optics. Excellent performance has been demonstrated down to the 70 nm 1:1 line/space level with focus latitude exceeding 1 μm and dose latitude of $\sim$10%. Moreover, dense-line printing down to a resolution of 50 nm has been achieved using resolution-enhancing pupil fills.

II. SYSTEM CONFIGURATION

Although the illumination partial coherence issue is the most fundamental of the changes required to implement printing in the EUV interferometry experimental station, several other modifications were necessary. These modifications have been previously described in detail[12] and include a modified optical path to support reflection reticles, increased wafer-stage speed to enable the acquisition of focus-exposure matrices in a reasonable amount of time (13×13 matrix in approximately 1 h), an electrostatic chuck for the wafer, and a vacuum load-lock wafer-transfer system. Many of these components serve dual interferometry and imaging roles such that only relatively minor modifications are required to actually switch between the two modes.

Description of the interferometry configuration is beyond the scope of this article, however, it has previously been described in detail.[4] As stated above, illumination coherence was the most fundamental concern for implementing lithographic printing capabilities on a beamline optimized for high spatial coherence. Working at the interferometry beamline[7,8] is analogous to performing conventional lithography using coherent laser illumination. We have addressed the partial-coherence issue by implementing an active illumination system.

In this illuminator, a spherical mirror is used to reimage a two-directional angular scanning mirror that serves as the effective source; thus it is a *critical* illumination system. The spatial-frequency content of the effective source is defined through control of the angular scan range. Analogous to the relationship between temporal coherence and spectral width, spatial coherence properties of a source are simply related to the Fourier transform of the source spatial spectrum.[13] Thus, it is evident that the illumination coherence properties can be directly controlled through the definition of the source scanning. Noting that the pupil fill is simply a representation of the source angular spectrum, the scanning described above is tantamount to painting out a desired pupil fill.

By definition, coherence is a time-integrated effect. In order to achieve the expected coherence function using the scanning method described above, the observation time (i.e., resist exposure time) must be long relative to the scan rate. In

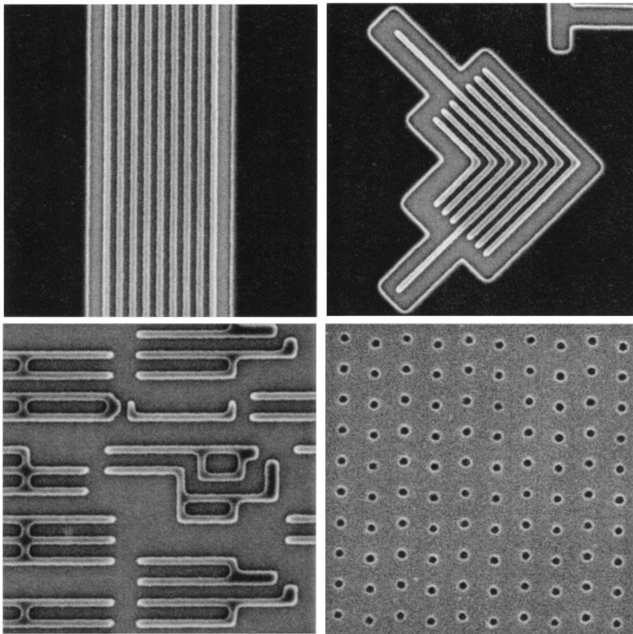

FIG. 3. Series of printed images at the Set-2 optic design CD of 100 nm. With a NA of 0.1, 100 nm CD represents a k_1 factor of 0.75. All images are recorded with conventional disk illumination and a partial coherence in the 0.7–0.8 range.

practice, this means that the lithographic exposure should last for at least as long as it takes to fully scan the desired pupil fill once. Additionally, the exposure time should be an integer multiple of the full pupil fill scan time in order to prevent nonuniform weighting within the pupil fill.

For the system presented here generating a disk pupil fill with σ=0.7, the elemental scan time is approximately 1 s, limited by the 80 Hz mechanical resonance of the two-dimensional (2D) scanner. In practice, we cycle through the pupil fill at least four times for improved uniformity; thus, a typical exposure is 4 s long. To support this relatively long scan time, the beamline power is intentionally restricted; unrestricted, the undulator beamline would support millisecond exposures in the 100 μm microfield.

Figure 1 shows a series of EUV pupil fills generated by the scanning system described above. The images were recorded using an integrating charge coupled device (CCD) positioned to effectively image the pupil. This back-thinned back-illuminated EUV CCD is the same detector used for interferometry. Pupil images can only be recorded when no imaging wafer is installed. The dashed lines in Fig. 1 represent the full 0.1 numerical aperture (NA) ETS optic pupil. These images demonstrate the wide variety of pupil fills (co-

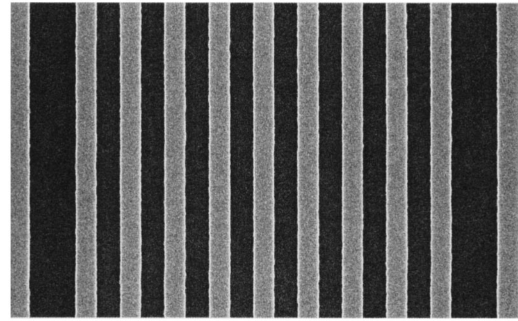

FIG. 4. Scanning-electron microscope image of 100 nm coded line/space pattern on 4×EUV mask.

herence functions) that can be generated. An important benefit of this illuminator is its ability to model pupil fills used in other systems. This level of control allows the microfield exposure tool presented here to not only characterize the imaging performance of the lithographic optic but also to investigate illuminator-specific effects. For example, implementing the ETS six-channel pupil fill (Fig. 1), enables more complete evaluation of the expected ETS performance.

III. LITHOGRAPHIC EVALUATION OF THE ETS SET-2 OPTIC

The static exposure system described above has been used to characterize ETS Set-2 optic. This optic will subsequently be installed into the ETS prototype full-field EUV stepper. The Set-2 optic is a 0.1 NA optic intended for 100 nm critical dimensions (CD).[5] At the central field point, where all subsequent printing results are presented, the optic was interferometrically measured to have a 37-Zernike wave front quality of 0.69 nm or 52 mwaves.[14,15] Using the wave front measured at wavelength, Fig. 2 shows the calculated binary-dense-line modulation transfer function (lower line) assuming a partial coherence of 0.7. Other than the global reduction in contrast due to flare, comparison with an ideal 0.1 NA optic (upper line) indicates that the optic should perform at the diffraction limit, at least in terms of the modulation transfer function. An initial rolloff is evident slightly below 100 nm CD with a much sharper rolloff starting around 70 nm CD. Although initially intended for 100 nm CD, it is evident that this optic should perform down to the 70 nm level using conventional illumination.

Figure 3 shows a series of representative images of 100 nm features recorded using conventional disk-fill illumination with a coherence factor in the 0.7–0.8 range. The wide exterior space in the lines/space image in Fig. 3 and all sub-

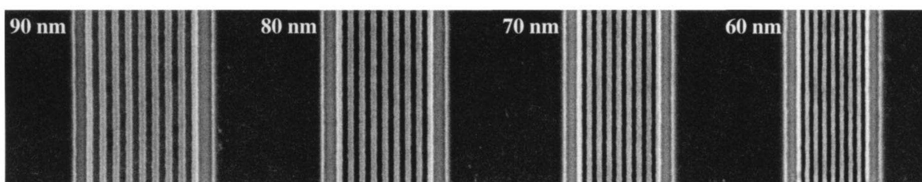

FIG. 5. Series of dense-line images ranging from 90 nm CD to 60 nm CD. All images were recorded with conventional disk illumination and a partial coherence of 0.8.

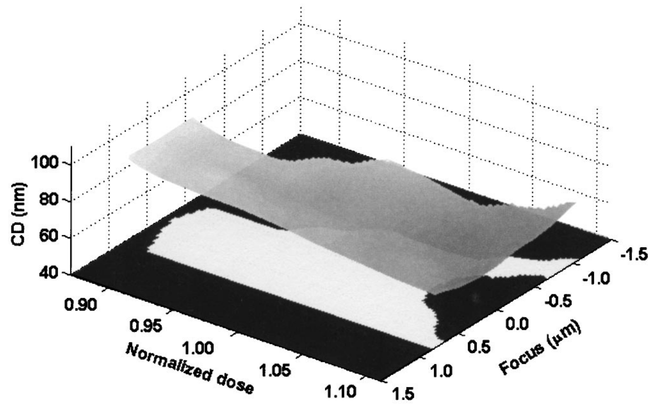

FIG. 6. Surface plot of the printed CD as a function of dose and focus overlain on a 2D map of all points falling within the ±10% CD range. Maximum rectangle fitting within this area at a dose latitude of 10% yields a depth of focus of 1.15 μm.

sequent figures is as written on the mask (Fig. 4). Based on the NA of 0.1, 100 nm CD corresponds to a k_1 factor of 0.75, where k_1 is defined as (CD)(NA)/λ. We note that extrapolating this performance to a NA of 0.25 with an equivalent wavefront quality yields a CD of 40 nm at the moderate k_1 factor of 0.75.

As indicated above, this optic is expected to perform down to the 70 nm level. Figure 5 shows a series of equal line-space images from 90 to 60 nm CD. All images were recorded with conventional disk illumination and a partial coherence of 0.8. Process window; studies based on ±10% CD change for 70 nm equal lines and spaces show a depth of focus of 1.15 μm with a dose latitude of 10%. Figure 6 shows a surface plot of the printed CD as a function of dose and focus overlain on 2D map of all points falling within the ±10% CD range.

As done in current photolithography, it is possible to decrease printed CD for loose-pitch features through dose control. Figure 7 shows 39 nm 3:1 pitch elbows printed by overdosing features coded as 80 nm 1:1 on the reticle. These results were obtained using conventional disk illumination with a partial coherence of 0.7. More challenging optically, however, is to reduce k_1 while maintaining a 1:1 pitch. The implementation of the custom-coherence illuminator described above enables the resolution of the system to be enhanced through the use of specialized pupil fills, such as dipole illumination (Fig. 1). Figure 7(b) shows a 50 nm equal line-space pattern printed using dipole illumination. This represents a k_1 factor of 0.37; the 0.25 NA equivalent would be 20 nm lines and spaces.

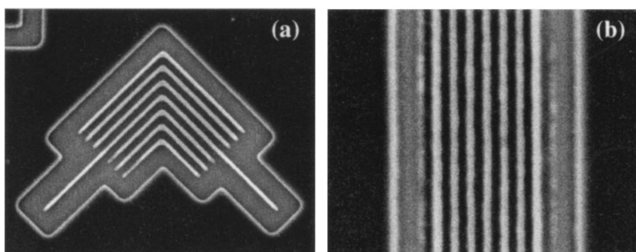

FIG. 7. (a) 39 nm 3:1 pitch elbows printed by overdosing features coded as 80 nm 1:1 on the reticle. Conventional disk illumination with a σ of 0.7 was used. (b) 50 nm dense line printing (k_1=0.37) achieved with dipole illumination.

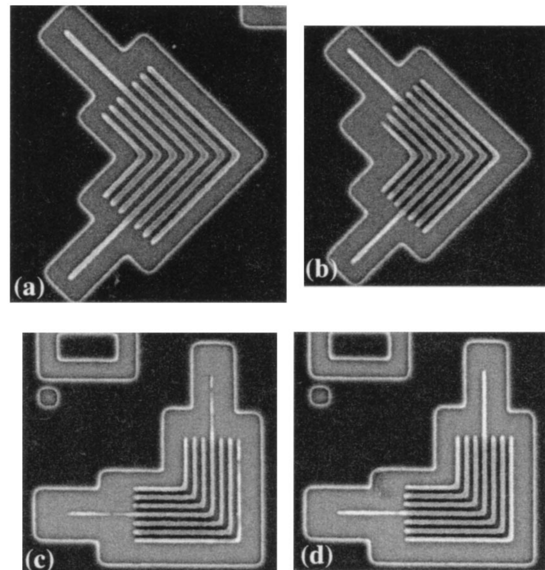

FIG. 8. 45° oriented elbow patterns printed with the ETS pupil fill with feature sizes of 80 nm (a) and 70 nm (b), and comparison of Manhattan geometry 70 nm elbows printed using ETS (c) and disk (d) pupil fills (σ =0.7).

Another important benefit of the scanning illuminator is its ability to simulate system-specific pupil fills such as the ETS six-channel pupil fill (Fig. 1). Figure 8 shows that although good performance is achieved down to 70 nm for certain orientations using the ETS pupil fill, increased horizontal–vertical bias limits the ability to print 70 nm scale feature in Manhattan geometry. Figures 8(a) and 8(b) show 80 nm and 70 nm 45° oriented elbow patterns printed with the ETS pupil fill, respectively, whereas Figs. 8(c) and 8(d) compare Manhattan geometry 70 nm elbows printed using ETS and disk pupil fills (σ=0.7), respectively. Preliminary results show the horizontal–vertical bias to be 17.4 nm for the ETS pupil fill and 9.7 nm for the disk fill. Part of the bias present in the ETS fill case and the majority of the bias present in the disk-fill case can be attributed to bias on the mask combined with a mask shadowing effect caused by off-normal mask illumination in a direction orthogonal to the horizontal features. This effect could be mitigated by properly biasing the mask.

IV. SUMMARY

Static microfield printing capabilities have been implemented at the EUV interferometry beamline at the Advanced Light Source synchrotron radiation facility at Lawrence Berkeley National Laboratory. These capabilities include a programmable coherence illuminator capable of *in situ* coherence control and arbitrary pupil fill synthesis for modeling alternative illuminators. The static microfield printing station

has been used to lithographically characterize the 0.1 NA ETS Set-2 optic. The Set-2 optic, which will be installed in the ETS, has demonstrated excellent imaging performance, well exceeding its intended specification of 100 nm CD. Using conventional illumination, 60 nm line printing on a 120 nm pitch has been demonstrated. Moreover, under resolution-enhancing dipole illumination, 50 nm line printing on a 100 nm pitch has been achieved. Characterization of the process window for 70 nm features revealed a 1.15 μm depth of focus with a 10% dose latitude based on ±10% CD change.

ACKNOWLEDGMENTS

The authors are greatly indebted to Kevin Bradley, Rene Delano, Gideon Jones, David Richardson, Ron Tackaberry, and Eugene Veklerov for expert engineering and fabrication support, and to the entire CXRO staff for enabling this research. This research was supported by the Extreme Ultraviolet Limited Liability Company and the DOE Office of Basic Energy Science.

[1]J. H. Underwood and T. W. Barbee, Jr., Appl. Opt. **20**, 3027 (1981).
[2]D. Atwood, G. Sommargren, R. Beguiristain, K. Nguyen, J. Bokor, N. Ceglio, K. Jackson, M. Koike, and J. Underwood, Appl. Opt. **32**, 7022 (1993).
[3]H. Medecki, E. Tejnil, K. A. Goldberg, and J. Bokor, Opt. Lett. **21**, 1526 (1996).
[4]K. A. Goldberg, P. Naulleau, P. Batson, P. Denham, H. Chapman, and J. Bokor, J. Vac. Sci. Technol. B **18**, 2911 (2000).
[5]D. W. Sweeney, R. Hudyma, H. N. Chapman, and D. Shafer, Proc. SPIE **3331**, 2 (1998).
[6]D. Tichenor *et al.*, J. Vac. Sci. Technol. B, these proceedings.
[7]D. Attwood *et al.*, IEEE J. Quantum Electron. **35**, 709 (1999).
[8]C. Chang, P. Naulleau, E. Anderson, and D. Attwood, Opt. Commun. **182**, 25 (2000).
[9]K. Itoh and Y. Ohtsuka, Opt. Commun. **31**, 119 (1979).
[10]K. Itoh and Y. Ohtsuka, Appl. Opt. **19**, 3184 (1980).
[11]V. Pol, J. Bennewitz, G. Escher, M. Feldman, V. Firtion, T. Jewell, B. Wilcomb, and J. Clemens, Proc. SPIE **633**, 6 (1986).
[12]P. Naulleau, K. Goldberg, E. Anderson, P. Batson, P. Denham, S. Rekawa, and J. Bokor, Proc. SPIE **4343**, 639 (2001).
[13]J. W. Goodman, *Statistical Optics* (Wiley, New York, 1986).
[14]P. Naulleau, K. Goldberg, E. Anderson, P. Batson, P. Denham, S. Rekawa, and J. Bokor, J. Vac. Sci. Technol. B **19**, 2396 (2001).
[15]K. Goldberg, P. Naulleau, J. Bokor, and H. Chapman, Proc. SPIE **4688**, 329 (2002).